

**ANOMALOUS DISPERSION PHASE-MATCHED SECOND HARMONIC
GENERATION IN POLYMER WAVEGUIDES: CHROMOPHORES FOR
INCREASED EFFICIENCY AND UV STABILITY**

T. Dai and K.D. Singer
*Case Western Reserve University
Department of Physics
Cleveland, OH 44106-7079*

R.J. Twieg
*Kent State University
Department of Chemistry
Kent, OH 44242*

T.C. Kowalczyk
*Gemfire Corp.
2471 E. Bayshore Road, Suite #600
Palo Alto, CA 94303*

Abstract

We report here on a series of tricyanovinylaniline chromophores for use as dopants in poled poly(methyl methacrylate) waveguides for anomalous dispersion phase-matched second harmonic generation. Second harmonic generation measurements as a function of mode index confirmed anomalous dispersion phase-matching efficiencies as large as $245\%/W\text{cm}^2$ over a propagation length of about $35\ \mu\text{m}$. The waveguide coupling technique limited the interaction length. The photostability of the chromophores was measured directly and found to qualitatively agree with photodegradation observed during second harmonic measurements over time and was found to be improved over previously reported materials. Prospects for obtaining efficient conversion by combining anomalous dispersion with Cerenkov phase matching are discussed.

I. INTRODUCTION

The generation of new optical frequencies using nonlinear interactions has been a topic of considerable interest. Generation of ultraviolet (UV) light using optical second harmonic generation has been of particular interest due to potential uses for optical data storage, xerography, photolithography, spectroscopy, and display applications. Organic and polymeric materials have shown promise in this area^{1,2,3}.

Waveguided second harmonic generation⁴ can produce efficient frequency conversion by phase-matching over long interaction lengths, using large fundamental intensities observed in waveguide confinement, employing materials with large optical nonlinearities, and operating in regions of low optical loss. Phase-matching, which can be challenging to effectively achieve in waveguided interactions, may introduce additional difficulties in providing mode overlap as in modal dispersion phase-matching and require phase matching of smaller off-diagonal second harmonic coefficients⁵.

A number of approaches to phase-matching have been employed in both inorganic and organic materials. These techniques include modal dispersion phase-matching,^{6,7,8} quasi-phase matching^{9,10,11}, and Cerenkov phase matching^{12,13,14}. In all of these techniques, materials that are transparent throughout the harmonic to fundamental wavelength range reduce the useful optical nonlinear susceptibility due the transparency-efficiency trade-off.¹⁵ This trade-off arises from the fact that in the conventional situation, the lowest lying absorption of the chromophore lies at higher energy than the second harmonic photons, thus limiting the magnitude of the nonlinear response. In anomalous dispersion, the lowest lying chromophore absorption lies between the fundamental and second harmonic energies. This allows utilization of the large optical nonlinearities found in visible absorbing dyes.

For anomalous-dispersion phase-matched second harmonic generation^{16,17}, a chromophore with absorption maximum between the fundamental and harmonic wavelengths is placed in a host polymer that exhibits normal dispersion. At an appropriate chromophore concentration, the normal dispersion of the host is canceled by the anomalous dispersion of the chromophore, yielding equal refractive indices at the fundamental and harmonic wavelengths. ADPM has several merits compared to the

conventional methods of phase-matching: exploitation of large diagonal second harmonic coefficients, high spatial overlap in matching lowest order modes, and defeat of the nonlinearity transparency trade off.¹⁵ In waveguides, the phase-matching can also be tuned by adjusting the thickness, and thus the mode index.

In our previous work, we demonstrated anomalous dispersion phase-matching in a polymer waveguide using a thiobarbituric acid (TBA) derivative¹⁶. These dyes are 4-amine donor substituted styrenes with a thiobarbituric acid acceptor group at the β,β terminus of the styrene. In that work, we observed efficient harmonic generation per unit length. However, absorption and the prism coupling technique limited the interaction length, and the second harmonic output was unstable due to photodegradation of the dye caused by the generated second harmonic light. The two related issues of reducing residual absorption and enhancing photostability must be addressed to make the use of anomalous dispersion practical, and we describe two approaches here. First, we report on the use of new tricyanovinyl (TCV) substituted chromophores possessing larger nonlinear optical susceptibilities and enhanced UV photostability. These dyes are amine-substituted styrenes with three cyano groups on the α,β,β positions of the styrene. These chromophores have recently been demonstrated in femtosecond pulse applications.¹⁸ Because UV photostability is more critical in waveguided applications, we also report here on the UV photostability as well as on the performance of the new materials in waveguided parametric devices in order to confirm whether photostability of the dye is responsible for the observed decay of second harmonic generation. Simple benzene based chromophores with TCV acceptors were among the first to be studied. Their large nonlinearities are well known.^{19,20} Second, we report how the combination of anomalous dispersion and Cerenkov phase matching may be employed to address the issue of absorption-limited propagation length and possibly to some extent photodegradation.²¹

II. MATERIALS

Nonlinear optical chromophores possessing enhanced properties for ADPM including better transparency at the harmonic wavelength, larger nonlinear optical

susceptibility, and enhanced UV photostability were synthesized. A range of simple tricyanovinylaniline chromophores which differ in the identity of the amine substituents were prepared and from this group three representative candidates were chosen which were readily compatible with PMMA.

The three tricyanovinyl substituted chromophores **1-3** used in this work are depicted in Figure 1 along with the previously studied thiobarbituric acid (TBA) derivative **4**. The substituents on the amine adjust various properties of the chromophores as we will show in this paper. Here the TCV compounds differ only in the respective groups on the donor nitrogen atom: a pair of 2-methylbenzyl groups in **1**, a cyclic pentamethylene group in **2** and a pair of n-butyl groups in **3**. All three TCV derivatives were prepared by the conventional method of reaction of a dialkylaniline with tetracyanoethylene.²² The N,N-bis(2-methylbenzylamino)aniline precursor for chromophore **1** was made by simple alkylation of aniline with 2-bromomethyltoluene. The combination of amine donor and tricyanovinyl acceptor moieties provide for a broad long-wavelength absorption and a large nonlinear optical susceptibility.²⁰ The UV-visible absorption spectra of the four compounds are shown in Figure 2. It is clear that the tricyanovinyl compounds exhibit significantly lower absorption in the harmonic region near 400 nm wavelength relative to analogous system with a thiobarbituric acid acceptor. This is the so-called “blue window” in the absorption spectra which lies between the charge transfer band (400 – 600 nm) and the higher energy aromatic electronic transitions (400 nm and lower, off scale in Figure 2). Table 1 lists the molar absorptivities in the blue “transparency window” for the chromophores considered here as well as the 1/e propagation length at the second harmonic wavelength. Three tricyano chromophores exhibit considerably lower absorption at the harmonic wavelength compared to TBA.

III. SAMPLE PREPARATION

The polymethylmethacrylate (PMMA) host polymer and dye were mixed to the desired weight fraction and dissolved in a mixture of solvents consisting of 65% propylene glycol methyl ether acetate (PGMEA) and 35% γ -butyrolactone (GBL) to a solid weight fraction of 8% -10%. Planar nonlinear optical waveguides were fabricated using a film float-off technique as we now describe. Indium tin oxide (ITO) glass coated substrates

were coated with the water soluble polymer polyvinylalcohol (PVA) release layer by spin-casting. The PVA solution was 5% solid weight fraction in deionized water with typical film thickness are around 0.5-2.0 μm . These films were placed in an oven for 30 minutes to eliminate water. Nonlinear optical waveguides were then spun onto PVA coated ITO glass using the spin speed and solution viscosity to control sample thickness. After spinning, films were placed in an oven for several hours at 80-90° C to remove solvent.

To produce the non-centrosymmetric ordering necessary for second order nonlinearities, the samples were corona poled on ITO glass.²³ A grid was inserted into the poling apparatus to control the magnitude and homogeneity of the poling field and to minimize the poling induced damage. Poling fields were measured with an isoprobe electrostatic voltmeter after poling. Following poling, films were then floated free by immersing the substrate and films in water to dissolve the PVA.¹¹ The freely suspended films were then used as planar waveguides.

IV. FILM CHARACTERIZATION

In order to determine the optimum (phase-matching) thickness of the waveguides for ADPM, we measured the dispersion of the refractive index of the films. This, along with the thickness, was used to determine the mode index dispersion. We employed a prism-coupling technique to precisely measure the refractive index. Free-standing films were applied to base of equilateral SF-10 glass dispersing prisms (Melles Griot Corporation) and the input coupling angle was tuned to obtain the effective index necessary to launch light into the waveguide. Guided modes were detected as dips in the intensity vs. input coupling angle scan and their locations were used to calculate bulk refractive indices.²⁴ The wavelength was tuned in the fundamental and harmonic regions using a tunable CW Ti:Sapphire laser and its second harmonic obtained with a frequency doubling lithium borate (LBO) crystal. Figure 3 shows the measured refractive indices and resulting fits to the following Sellmeier equation using the absorption maximum wavelength and oscillator strength obtained from UV-visible absorption measurements:

$$n = \sqrt{1 + \frac{A_0 I^2}{I^2 - I_0^2} + \frac{A_1 I^2}{I^2 - I_1^2} + \frac{A_2 I^2}{I^2 - I_2^2}} . \quad (1)$$

Fit parameters are listed in Table 2.

In waveguides, it is the effective refractive index that must be phase-matched. We calculated the effective index of the poled films as a function of waveguide thickness in order to predict the phase-matching thickness.²⁴ Figure 4 depicts the effective index as a function of waveguide thickness for the lowest order fundamental and harmonic TM modes. The intersection points indicate phase-matching film thickness. Experimentally it is possible to tune through the phase-matching condition by varying the film thickness. Based on the results in Figure 4, a series of films of various thicknesses were prepared near the phase-matching thickness in order to verify the phase-matching properties.

The second harmonic coefficients of thin films containing each chromophore was determined by the rotational Maker fringe method²⁵ in transmission using a previously described method.²⁶ The fundamental at 1340 nm wavelength was produced by an optical parametric oscillator pumped with the second harmonic of a nanosecond pulse Nd:YAG laser. The beam was passed through a polarizer and then was split into sample and reference beams. The reference beam was focused onto a quartz plate resulting in second harmonic light that was collected with a photomultiplier tube, and was used to eliminate shot-to-shot fluctuations in the pulsed laser. In the sample arm, light was focused onto the sample and the second harmonic was measured as function of sample rotation angle. The experiments allowed the nonlinearity to be determined with respect to the nonlinearity of a known quartz reference sample ($d_{11}=0.486$ pm/V) as measured in a subsequent run. The data analysis has been described earlier, and assumes, as is usual for nonresonant measurements, that the film thickness is much less than the coherence length.²⁶ Results are given in Table 3 along with values normalized to the poling field.

VI. ADPM SECOND HARMONIC GENERATION

A femtosecond modelocked Ti: sapphire laser was constructed to measure the conversion efficiency. This laser is advantageous because it has a high repetition rate (100MHz), high peak power pulses from 100fs mode-locked pulses, and its tuning capabilities allowed frequency doubling into the short wavelength transparency window of

the ADPM chromophores. Fundamental laser light was focused onto the coupling spot of the free film on the base of an equilateral prism using a lens of focal length 12.5 cm. The prism was angle-tuned to selectively couple into the lowest order synchronous angle and the reflected fundamental was attenuated with a neutral density filter and collected on a large area calibrated silicon detector.

The coupling efficiency can only be roughly estimated, and represents the largest uncertainty in the accuracy of the measured efficiency. The tight focusing of the incident beam results in an m-line whose thickness is much less than the beam spot reflected from the prism base. Thus, most of the beam may not be coupled in. We measured the reflected intensity with two detectors: one whose area is much larger than the reflected spot, and one whose dimension matches the width of the m-line. We found that the reflected power dipped by 5% when turning through the m-line with the large detector, and by about 30% with the small detector. This confirms that most of the light is not coupled in due to the angular spread caused by the relatively tight focus. We assumed the 5% dip included both the tunneling efficiency and the losses due to angular spread. We assumed that the outcoupling efficiency is unity. The outcoupling efficiency is probably lower, but we wished to err on the side of underestimating the conversion efficiency. We multiplied the incoming fundamental power by 0.05, and the outgoing second harmonic power by 1 to determine the efficiency given in Table 3. We should note that the effect of the uncertainty of the coupling efficiency would affect the accuracy much more than the comparative numbers since we observed the same coupling factors for each sample. In addition, we have attempted to state the conversion efficiencies conservatively.

The average power was taken to be the incident fundamental power. The temporal pulse width was measured with an autocorrelator giving a duration of 96 fs. From this and the measured repetition rate, the peak power of the pulses was determined. The experimental conversion efficiency was defined as the ratio of peak (pulsed) harmonic power to the peak fundamental power with coupling corrections as described above. Results for peak conversion are given in Figure 5 and Table 3. The relative amount of second harmonic power is plotted versus film thickness. The data was fitted to

$$I = C \operatorname{sinc}^2\left(\frac{\Delta kL}{2}\right) \quad (2)$$

using the amplitude C and the propagation length L as adjustable parameters. Both C and L could be robustly fit since C largely determines the amplitude (related to the conversion efficiency) and L the width of the curve yielding the propagation length listed in Table 3. Note that the values of L listed in Table 3 are much less than the absorption lengths l listed in Table 1 so that the approximation of low absorption implicit in Eq. 2 is reasonable. Additionally, it is clear that the propagation length and thus the efficiency is limited by the prism coupling technique rather than absorption.

VII. PHOTOSTABILITY

Photostability is a critical material parameter for device lifetime, especially in parametric interactions where multiple wavelengths are simultaneously used and generated. While it is often desirable for these devices to operate at high optical intensity to enhance nonlinear interactions, these conditions also may also provide additional pathways for photochemical damage that include single and multiple-photon interactions. Harmonic generation into the UV, in particular, tests the limit of dye photostability because energetic photons can cause bond delocalization or simply dye ablation or bleaching that ultimately lead to device failure. Until recently, photostability has been ignored as a key material parameter in favor of nonlinearity, transparency, and thermal/temporal stability of induced nonlinearity. In our previous work we observed a strong decay of harmonic generation conversion over time that was attributed to dye decomposition.¹⁶ In this study we probed the photostability of dye molecules using SHG experiments, UV photobleaching (in the blue transparency window), and a pump-probe experiment to determine quantum efficiencies of photodegradation. The technique was used to yield quantitative values for dye photostability as it relates to chemical structure.

In the first of these experiments, the second harmonic signal was observed to decay over time as shown in Figure 6. First, Figure 6a depicts the conversion efficiency changes as a function of time at the maximum conversion efficiency. The maximum conversion efficiency was scaled to unity at $t=0$. After 4 minutes' exposure, the conversion efficiency of the waveguides containing the three tricyanovinyl substituted chromophores

decreased to around 50%, while at the same time the efficiency of the waveguide containing the TBA decreased to around 22% even though it generated approximately an order-of-magnitude less UV light. This decay is likely due to the combination of lower photostability and higher absorption at the second harmonic wavelength. Second, to eliminate differences in harmonic light power that were attributed to conversion efficiency differences, decay data was collected for all samples operated at the same 25% conversion efficiency for each compound as shown in Figure 6b. The efficiency was adjusted by phase-matching, i.e. by using a film of appropriate thickness. Figure 6b shows that under relatively similar UV fluence conditions, TCV dyes decayed to around 80% of their original value whereas TBA decayed to approximately 20%.

Photobleaching of the chromophores was studied directly in these polymer films by flood exposure with a broadband medium pressure Hg vapor UV-light source that provided 32 mW/cm² of 365 nm wavelength light. The light source was sufficiently large and homogeneous so that all samples were bleached simultaneously. Absorbency changes at λ_{max} were monitored as a function of exposure time in an ambient (oxygen containing) environment using a UV-visible spectrometer. Figure 7 shows the changes in absorbency resulting from 365 nm UV flood exposure. The absorption maximum was scaled to unity at t=0. For the three tricyanovinyl-substituted chromophores, dye bleaching is slow compared to the dye bleaching of TBA. Nearly all of the TBA dye was photobleached after 5 minutes of UV exposure. Only 25% of TCV dye **2** was photobleached after an hour of exposure while the other TCV dyes **3** and **1** remained relatively stable after one hour of exposure. This is considerably longer than the waveguide results due to the fact that the intensity is considerably lower in the flood exposure case. Although not shown here, similar tests performed in a N₂ environment resulted in substantially improved dye photostability for compound **2** and TBA. For the case of dye **2** at most 7% of the dye was lost after one hour, suggesting that oxygen plays a significant role in the photodegradation process, perhaps through singlet oxygen excitation. Although approximately 70% of TBA decomposed after one hour of UV-exposure, it also exhibited enhanced photostability in a nitrogen environment.

Photostability was also characterized using a pump-probe laser method to monitor changes in the electronic absorption band as detected by transmission changes of a 543nm probe beam as a function of pump laser fluency. This experiment is beneficial for quantitatively comparing different dyes because it yields an intrinsic photostability parameter, quantum efficiency for photodegradation (average number of photons a dye molecule can absorb before decomposition), that is obtained by fitting a theoretical expression containing only one adjustable parameter. Figure 8 shows an illustration of the experiment. A sputtered thin-film metal mask containing 100 μ m apertures was fabricated on each sample to define exposure regions for the experiment. Although the experiment allows for different pump and probe wavelengths, the results in this paper represent the degenerate case of $\lambda_1=\lambda_2=543\text{nm}$.

For modeling experimental results and determining intrinsic photostability a simple one-photon process was used to describe the absorption characteristics of the dye-doped polymer samples. Further, assuming that decomposition products absorb less than unbleached dyes and that the dye is randomly distributed in the polymer matrix, an expression relating %-transmission changes to integrated pump energy can be developed.²⁷ The expression takes the form

$$T(E) = T_{\infty} / [1 + (T_{\infty}/T_0 - 1) \exp(-\beta E)] \quad (3)$$

where

$$T_0 = \exp(-\sigma_1 J_0), \quad T_{\infty} = \exp(-\sigma_2 J_0), \quad \text{and} \quad \beta = \sigma_1 / h\nu B$$

where $T(E)$ is the probe beam transmission as a function of input energy, T_{∞} is the probe beam transmission for a nearly bleached sample (time = infinity), T_0 is the probe beam transmission at the start of the experiment, σ_1 and σ_2 are the absorption cross-sections of the dye and bleached species respectively, J_0 is the number of dye molecules per unit area, h is Planck's constant, ν is the frequency of light, and B^{-1} is the quantum efficiency for photodegradation. Because the initial and final transmission values are extracted from the experiment, the only remaining unknown parameter, B , is used as an adjustable parameter to fit the data. Figure 9 shows pump-probe photostability data of a TBA/PMMA sample at 543nm. A B -value of 0.3×10^6 was used to fit equation (3) to the experimental data. After approximately 1 J of integrated 543nm optical energy, TBA is almost completely

decomposed. Once a device geometry is specified and failure limits identified, lifetimes of dye-doped systems limited by photostability can be extrapolated from plots similar to Figure 9.

Results are listed in Table 4. Larger B-values indicate better photostability. Compounds **1**, **2** and **3** differ only in donor substitution in the amine group and result in only slight changes in photostability, TBA on the other hand has considerably less photostability. The appropriate figure-of-merit for describing photostability of dye systems must include the absorption characteristics of the dye at the measurement wavelength. For this reason we have listed the photostability FOM in Table 4. TCV dyes are among the most photostable EO dyes that have been measured thus far.

DISCUSSION

Table 3 contains the major results concerning ADPM second harmonic generation. Conversion efficiencies are reported for peak power since power density is difficult to determine in slab waveguides, and the power efficiency is more relevant in applications. Extremely large conversion efficiencies per unit length are obtained with the new tricyanovinyl substituted chromophores. These figures are the largest reported thus far and confirm the efficacy of ADPM, in particular, the ability to exploit the second harmonic coefficients of visible absorbing chromophores. Obviously, the tricyanovinyl dyes are an improvement over the previously studied TBA compound.

The relatively constant value of the last column of Table 3 indicates that the second harmonic coefficient determines the conversion efficiency and that the coupling and phase-matching properties are similar from film to film. This can be explained by the fact that the propagation length is relatively constant from film to film and is mainly determined by the single prism coupling technique rather than the absorption length. As stated previously, the absorption length ($1/e$) is much longer than the propagation length in all cases.

Inspection of Figures 6b, 7 and Table 4 indicate that photobleaching of the dyes in the waveguide could be a major contribution to the decay of conversion efficiency. The second harmonic light generated in the guide that is adsorbed by the dye may lead to

degradation of the chromophore due to simple loss of bulk second order nonlinearity. Also, there may be other secondary damage mechanisms that produce losses in the guide due to other processes. The trends in all three measurement techniques are consistent and indicate enhanced photostability in the tricyanovinyl dyes.

It is difficult to provide any detailed mechanistic interpretation here concerning the relative performance and stability among the three TCV dyes. The various electrooptic and efficiency values for the three TCV dyes are, in fact, quite similar as seen from the values in Table 1. As far as stability goes, the TCV chromophores again differ little but the observed trend is **1** > **3** > **2**. It is interesting to note that this is the same trend as observed for the thermal stability for these three dyes with the following respective onset (T_{di}) and maximum (T_{dm}) of decomposition in deg C measured at 20 deg/min for **1** (356, 373), **2** (318,329), **3** (349, 392).^{28,29} With a larger and more diverse set of TCV chromophores with more disparate structures one might be able to establish some clear-cut relationships amongst performance characteristics such as photochemical stability and thermochemical stability and molecular characteristics such as oxidation potential and optical adsorption (energies of the electronic transitions). Typical more disparate examples of TCV dyes include the julolidine derivative, which should be more nonlinear but much less stable, and the dihenylamino derivative, which could possess even superior stability to the three TCV dyes examined here for ADPM applications.³⁰ It is clear that the tricyanovinyl dyes represent an improvement in the materials set available for development of the ADPM technique, and that ADPM leads to large conversion efficiency.

Further improvements in photostability are needed. However, both the problems of photostability and the propagation length problem due to absorption can be addressed by considering Cerenkov phase matching in conjunction with ADPM since the second harmonic does not propagate in the dye-doped waveguide, but rather in the transparent cladding. Figure 10 depicts the conversion efficiency of Cerenkov phase matching as a function of the intrinsic material dispersion. These results are based on the previously reported calculation.²¹ By using ADPM, one can move to the left along the curve and attain exponential increases in Cerenkov conversion efficiency. Further, as seen in the figure, Cerenkov efficiency is relatively insensitive to absorption since the second

harmonic is not confined in the waveguide. This technique will not eliminate all of the problems of photodegradation due to the residual UV absorption since high intensity locally produced SHG resides in the waveguide prior to launching radiation into the cladding, pointing to the need for further improvement in UV photostability.

Understanding the mechanisms of photochemical degradation is currently an active area of research. The Cerenkov/anomalous dispersion measurement will allow assessment of the potential of anomalous dispersion methods in practical second harmonic generation devices.

IX. CONCLUSIONS

We have investigated a series of tricyanovinyl chromophores as guest-host type polymer in PMMA. We demonstrated their high second harmonic generation conversion efficiency and improvements in the photochemical stability. The maximum conversion efficiency of 245 %/Wcm² and improved photostability has been demonstrated. Further improvement in UV stability and the use of other techniques such as ADPM enhanced Cerenkov could lead to the development of UV sources using this technique.

X. ACKNOWLEDGMENTS

The authors wish to acknowledge Dr. Paul Cahill of Exciton for providing the TBA samples. They are also grateful for support from the National Science Foundation (ECS95-21664).

References

- ¹ G.Khanarian, R.A.Norwood, D.Haas, B.Feuer, D.Karim, "Phase-matched 2nd harmonic generation in a polymer waveguide", *Appl. Phys. Lett.* **57**, 977-979 (1990).
- ² H.Yamamoto, T.Sugiyama, J.Jung, T. Kinoshita, and K. Sasaki, "Cerenkov-radiation and guided-mode blue second-harmonic generation in four-layer waveguides using organic thin-film crystals", *J. Opt. Soc. Am. B* **14**, 1831-1837 (1997).
- ³ K.D.Singer, W.R.Holland, M.G.Kuzyk, G.L.Wolk, P.A.Cahill, "Guest-Host Polymers for nonlinear optics", *Mol. Cryst. Liq. Cryst.* **189**, 123 -136(1990).

- ⁴ T.L.Penner, H.R.Motschann, N.J.Armstrong, M.C.Ezenyilimba, D.J.Williams, "Efficient phase-matched 2nd-harmonic Generation of blue-light in an organic waveguide", *Nature* **367**, 49-51 (1994).
- ⁵ W.Wirges, S.Yilmaz, W.Brinker, W. Bauer-Gogonea, S. Bauer, M. Jager, G.I. Stegeman, M. Ahleheim, M. Stahelin, B. Zysset, F. Lehr, M. Diemeer, and M.C. Flipse, "Polymer waveguides with optimized overlap integral for modal dispersion phase-matching", *Appl. Phys. Lett.* **70**, 3347-3349 (1997).
- ⁶ M.Jager, G.I.Stegeman, S.Yilmaz, W.Wirges, W.Brinker, S.Bauer-Gogonea, S.Bauer, M.Ahlheim, M.Stahelin, B.Zysset, F.Lehr, M.Diemeer, M.C.Flipse, " Poling and characterization of polymer waveguide for modal dispersion phase-matched second-harmonic generation", *J. Opt. Soc. Am. B* **15**, 781-788 (1998).
- ⁷ O. Sugihara, T. Kinoshita, M. Okabe, "Phase-matched 2nd harmonic generation in poled dye polymer waveguide", *Appl. Opt.* **30**, 2957-2960 (1991).
- ⁸ M. Jager, G.I.Stegeman, M.C. Flipse, M. Diemeer, and G. Mohlmann, "Modal dispersion phase matching over 7 mm length in overdamped polymeric channel waveguides", *Appl. Phys. Lett.* **69**, 4139-4141 (1996).
- ⁹ X.G.Huang, M.R.Wang, "A novel quasi-phase-matching frequency doubling technique", *Opt. Commun.* **150**, 235-238 (1998).
- ¹⁰ V.Taggi, F.Michelotti, M.Bertolotti, G.Petrocco, V.Foglietti, A.Donval, E.Toussaere, J.Zyss, "Domain inversion by pulse poling in polymer films", *Appl. Phys. Lett.* **72**, 2794-2796 (1998).
- ¹¹ M.A.Mortazavi, G. Khanarian, "Quasi-phase-matched frequency-doubling in bulk periodic polymeric structures", *Opt. Lett.* **19**, 1290-1292 (1994)
- ¹² N. Hashizume, T. Kondo, T. Onda, N. Ogasawara, S. Umegaki, R. Ito, " Theoretical analysis of Cerenkov-type optical second-harmonic generation in slab waveguides", *IEEE J. Quant. Electron.* **28**, 1798-1815 (1992)
- ¹³ Y. Chen, M. Kamath, A. Jain, J. Kumar, S. Tripathy, "Cerenkov-type phase-matched 2nd-harmonic generation in polymeric channel waveguides", *Opt. Commun.* **101**, 231-234 (1993)

- ¹⁴ T.K.Lim, M.Y.Jeong, S.N.Cha, E.K. Koh, and D.Y. Han, "Cerenkov-type second harmonic generation with a nonlinear organic polymer waveguide", *J. Korean Phys. Soc.* **30**, 544-549 (1997).
- ¹⁵ P.A.Cahill and K.D.Singer, "Chemistry of anomalous dispersion phase-matched 2nd harmonic generation", *ACS Symp. Ser.* **455**, 200-213 (1991).
- ¹⁶ T. C. Kowalczyk, K. D. Singer, and P. A. Cahill, "Anomalous-dispersion phase-matched second-harmonic generation in a polymer waveguide", *Opt. Lett.* **20**, 2273-2275 (1995)
- ¹⁷ R. Dietrich, K. Meerholz, C. Brauchle, J. Wichern, P. Boldt, "Phase-matched second harmonic generation due to anomalous dispersion: tailoring of the refractive indices in three-component systems", *Chem. Phys. Lett.* **280**, 119-126 (1997).
- ¹⁸ D.R. Yankelevich, P.Pretre, A.Knoesen, G.Taft, M.M.Murnane, H.C.Kapteyn, R.J.Twieg, "Molecular engineering of polymer films for amplitude and phase measurements of Ti:sapphire femtosecond pulses", *Opt. Lett.* **21**, 1487-1489 (1996).
- ¹⁹ J.B. Stamatoff, A. Buckley, G. Calundann, E.W. Choe, R. DeMartino, G. Khanarian, T. Leslie, G. Nelson, D. Stuetz, C. C. Teng, and H.N. Yoon, *Proc. SPIE* **682**, 85-96 (1986).
- ²⁰ H.E. Katz, K.D. Singer, J.E. Sohn, C.W. Dirk, L.A. King, and H.M. Gordon, "Greatly enhanced second-order nonlinear optical susceptibilities in donor-acceptor organic molecules", *J. Am. Chem. Soc.* **109**, 6561-6563 (1987).
- ²¹ T. C. Kowalczyk, K. D. Singer, and P. A. Cahill, "Anomalous-dispersion enhanced Cerenkov phase-matching", *Proc. SPIE* **2025**, 332-343 (1993)
- ²² B.C. McKusick, R.E. Heckert, T.C. Cairns, D.D. Coffman, and H.F. Mower, "Cyanocarbon Chemistry. VI. Tricyanovinylanilines" *J. Am Chem. Soc.* **80**, 2806-2815 (1958).
- ²³ K.D. Singer, M.G. Kuzyk, R.B. Comizzoli, H.E. Katz, M.L. Schilling, W.R. Holland, J.E. Sohn, S.J. Lalama, "Electro-Optic Effects and Second-Harmonic Generation in Corona-Poled Polymer Films", *Appl. Phys. Lett.* **53**, 1800-1802 (1988).
- ²⁴ P.K. Tien and R. Ulrich, "Theory of Prism-Film Coupler and Thin-Film Light Guides", *J. Opt. Soc. Am.* **60**, 1325-1337 (1970).

- ²⁵ J. Jerphagnon, S. K. Kurtz, "Maker Fringes: a detailed comparison of theory and experiment for isotropic and uniaxial crystals", *J. Appl. Phys.* **41**, 1667-1681 (1970)
- ²⁶ K.D. Singer, J.E. Sohn, and S.J. Lalama, "Second Harmonic Generation in Poled Polymer Films", *Appl. Phys. Lett.* **49**, 248-250 (1986).
- ²⁷ A. Dubois, M. Canva, A. Brun, F. Chaput, J.-P. Boilot, "Photostability of Dye Molecules Trapped in Solid Matrices", *Appl. Opt.* **18**, 3193-3199 (1996).
- ²⁸ R J. Twieg, unpublished results on TCV dye stability.
- ²⁹ R.B. Prime, G. Y. Chiou, R.J. Twieg, "Evaluation of the Thermal Stability of Some Nonlinear Optical Chromophores", *J. Therm. Anal.*, **46**, 1133-1150 (1996)
- ³⁰ T. C. Kowalczyk, R. J. Twieg, H. L. Lackritz, "Photochemical Stability of Electro-Optic Chromophores", *Poly. Prep.*, **39**, 1015 (1998).

Table 1. Absorptivity parameters for the studied dyes. The percent is dye percent by mass in the polymer film. The quantity ϵ_{\min} is the minimum molar absorptivity in the UV transparent region, ϵ_0 the peak molar absorptivity in the visible region with the corresponding wavelengths listed, and l the 1/e propagation length due to absorption.

Dye	MW au	λ_{\min} nm	λ_0 nm	ϵ_{\min}	ϵ_0	l (μm)
10% 1	403	355	492	170	51000	280
8% 2	262	361	503	220	55000	150
8% 3	306	363	507	90	49000	500
8% TBA	396	384	506	500	90000	120

Table 2. Fit parameters to the Sellmeier equation.

Dye	A_0	λ_0	A_1	λ_1	A_2	λ_2
10% 1	1.174	123	0.050	508	-934	2.36×10^5
8% 2	1.174	125	0.053	515	-424	2.47×10^5
8% 3	1.171	123	0.047	517	4.96	9.41×10^5
8% TBA	1.170	123	0.044	514	185	5.06×10^6

Table 3. Results of second harmonic generation measurements in poled polymer waveguides at the anomalous dispersion phase-matching peak. The quantity d_{33} is the second harmonic coefficient of the measured film determined from second harmonic generation, E_p the magnitude of the poling field, P the beam powers, L the interaction length, and η the guided-wave conversion efficiency.

Material	E_p MV/cm	d_{33} 10^{-12} m/V	d_{33}/E_p 10^{-12}	P^ω (ave) mW	$P^{2\omega}$ (ave) μ W	P^ω (peak) W	$P^{2\omega}$ (peak) W	L μ m	η %/Wcm ²	η/d_{33}^2 A.U.
10% 1	1.93	11.2	5.8	4.5	33	450	3.3	36.4	215	172
8% 2	1.85	10.6	5.7	3.5	17	350	1.7	34.7	203	181
8% 3	1.82	11.8	6.4	4.5	38	450	3.8	36.7	245	176
8% TBA	2.03	3.9	1.9	4.5	2.8	450	0.28	30.3	26.5	173

Table 4. Results of pump-probe photostability experiments. B represents the quantum efficiency for photodegradation (average number of photons a dye molecule can absorb before decomposition). Larger B-values indicated better photostability. The photostability parameter is the ratio B/σ .

Dye	Thickness μm	N $10^{20}/\text{cm}^3$	σ 10^{-16}cm^2	B @543nm 10^6	FOM 10^{16}cm^{-2}
1	0.91	1.42	0.9	3.0	3.3
2	1.43	2.19	1.0	1.0	1.0
3	0.96	1.87	1.2	1.5	1.25
TBA	1.67	1.10	0.6	0.3	0.5

Figure Captions

Figure 1. Nonlinear optical dyes used in this study.

Figure 2. Ultraviolet-visible absorption of the studied dyes as dissolved in PMMA films with maxima normalized to unity.

Figure 3. Refractive index dispersion of 10% weight fraction **1** in PMMA, 8% **2** in PMMA, 8% **3** in PMMA, and 8% TBA in PMMA. Solid lines are fits to a three-parameter Sellmeier equation.

Figure 4. Mode indices of the fundamental and second harmonic TM_0 modes versus thickness as calculated from index of refraction data.

Figure 5. Phase matching curves for guided wave second harmonic generation. Solid lines are fits to Equation 1 with the amplitude and phase mismatch as fitted parameters.

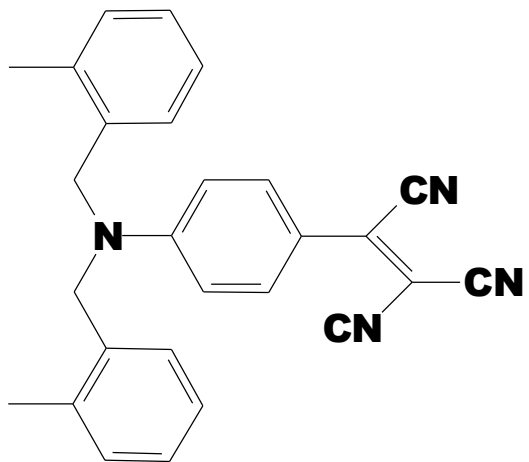
Figure 6. Conversion efficiency as a function of time for a) maximum conversion efficiency and b) at 25% conversion efficiency.

Figure 7. UV photobleaching of dyes.

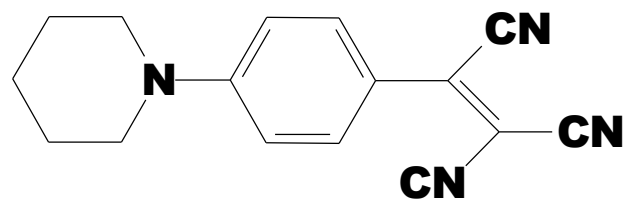
Figure 8. Photobleaching experimental setup.

Figure 9. TBA/PMMA pump-probe photostability experimental data and resulting fit to equation (1) using $B=0.3 \times 10^6$.

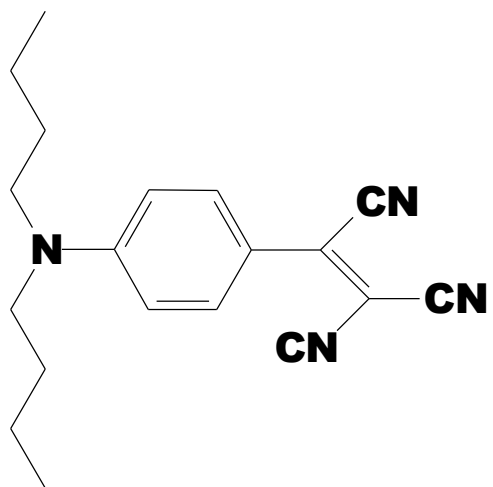
Figure 10. Theoretical conversion efficiency for Cerenkov phase matching versus bulk refractive index difference. Curves are parameterized by various absorption levels in the waveguide at the second harmonic wavelength.



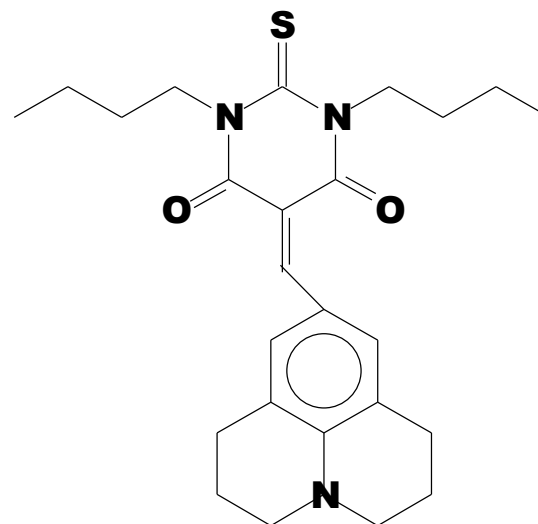
1



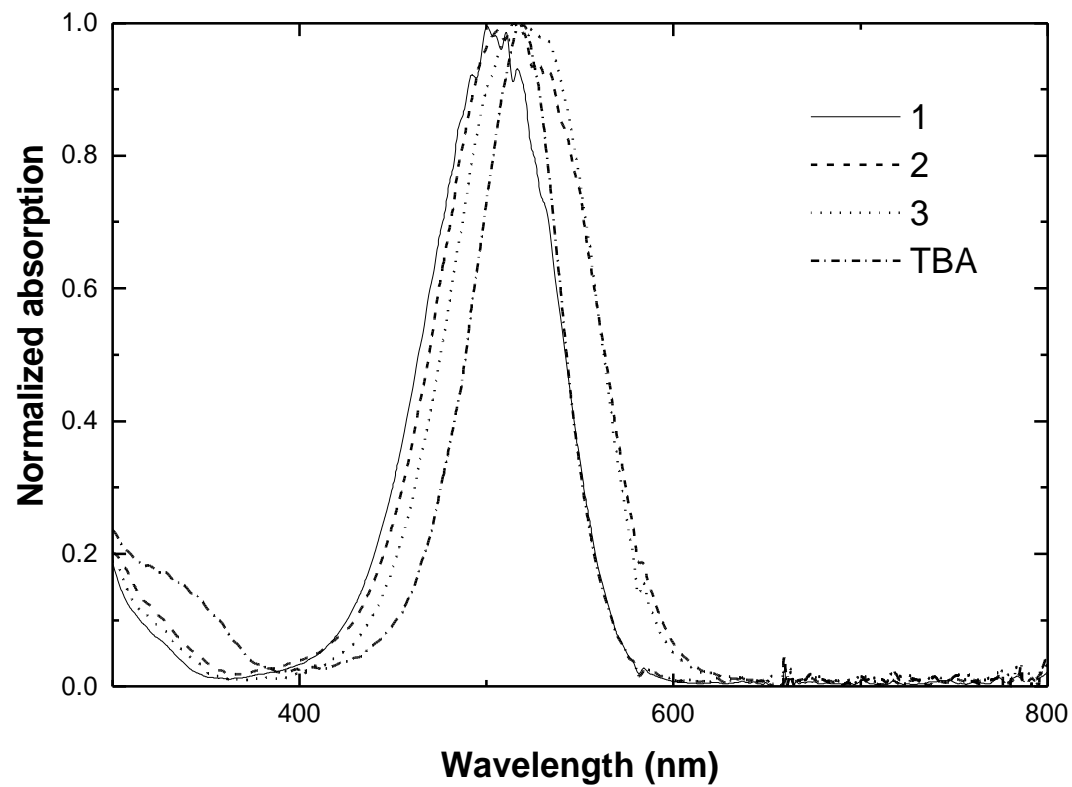
2

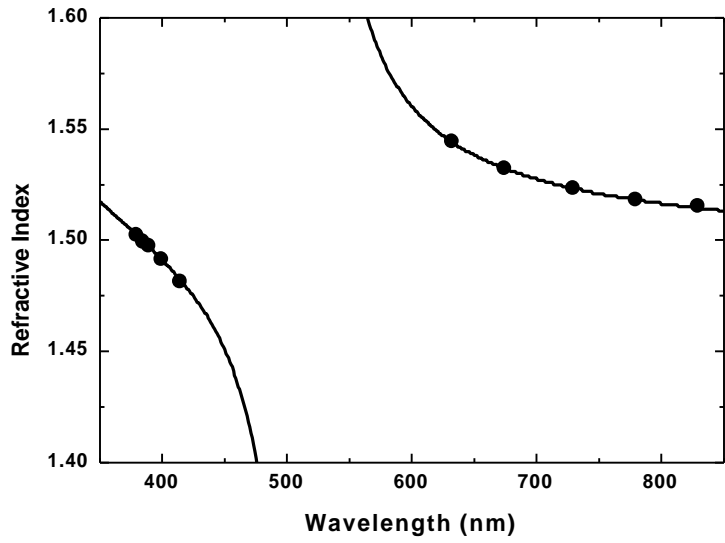


3

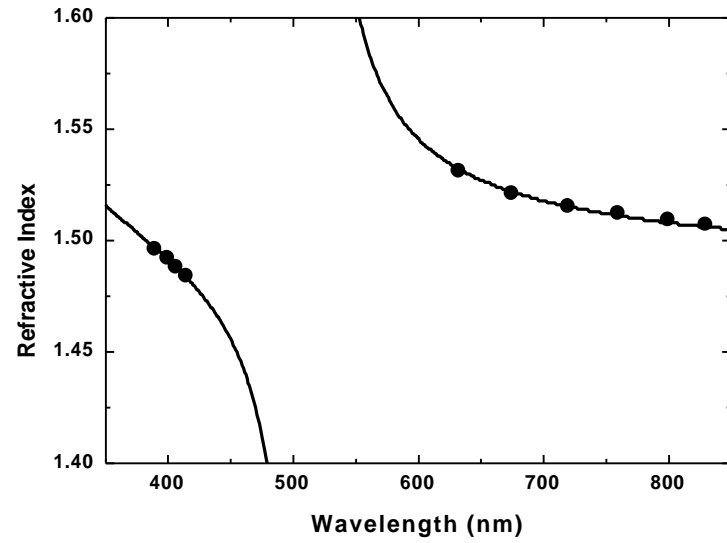


TBA

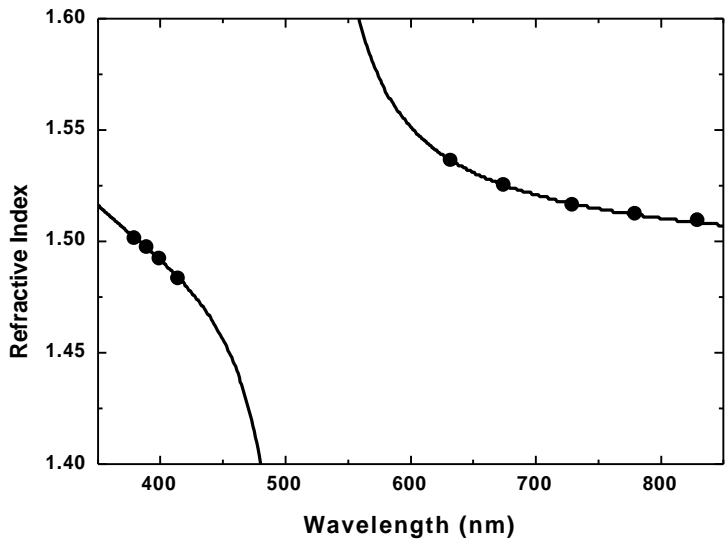




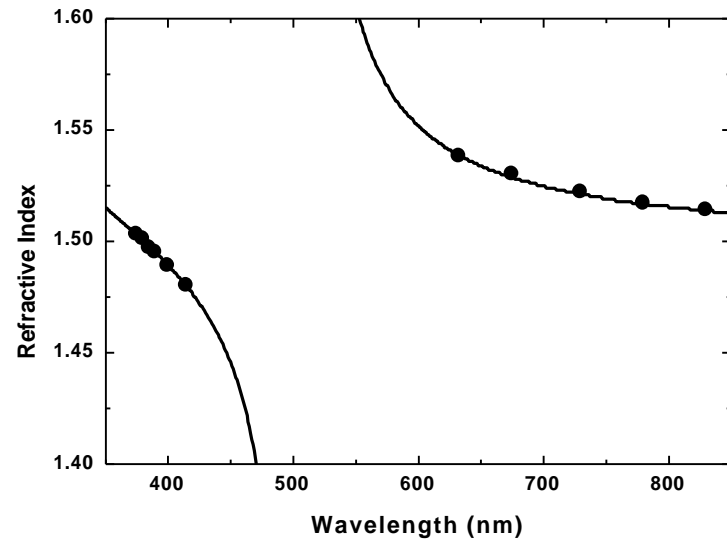
1



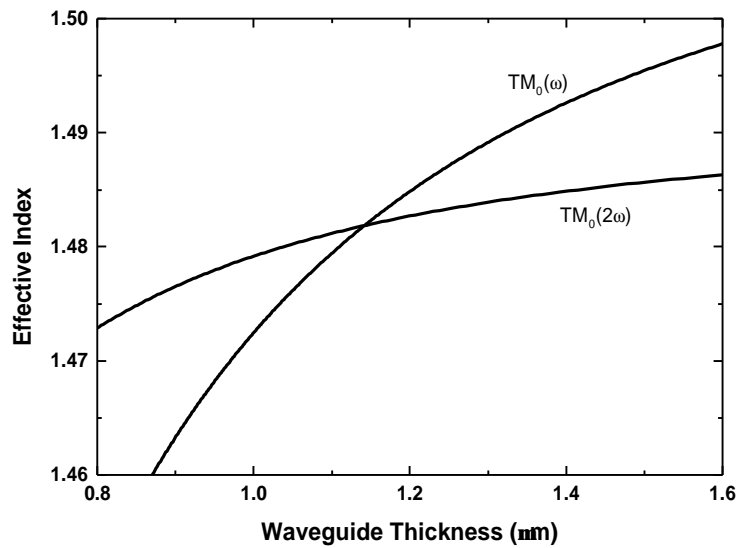
2



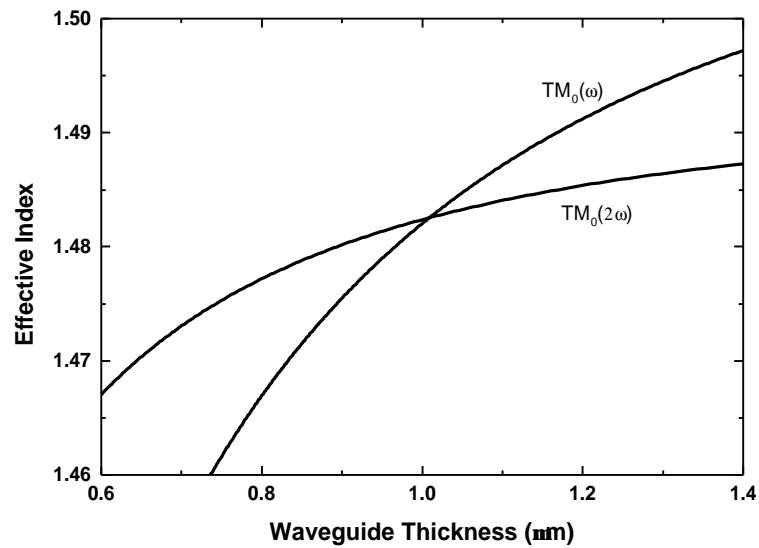
3



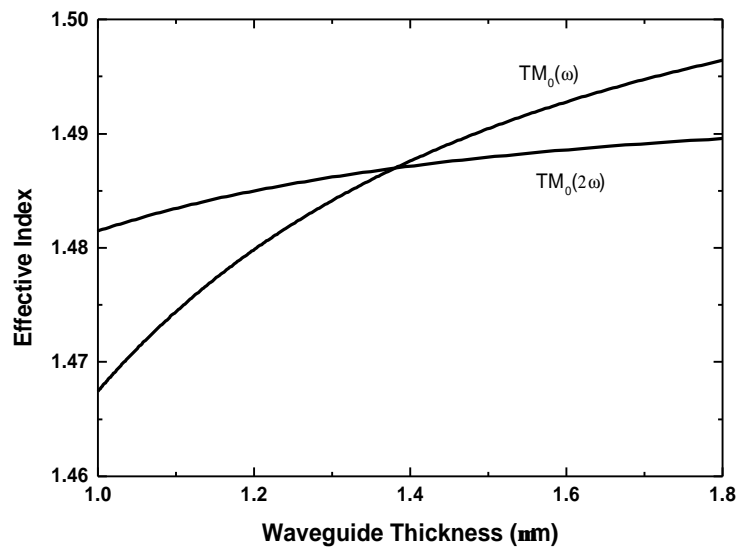
TBA



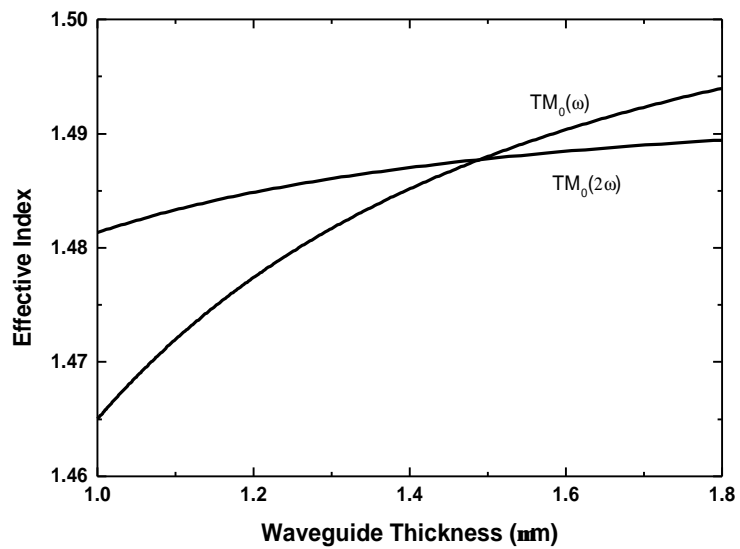
1



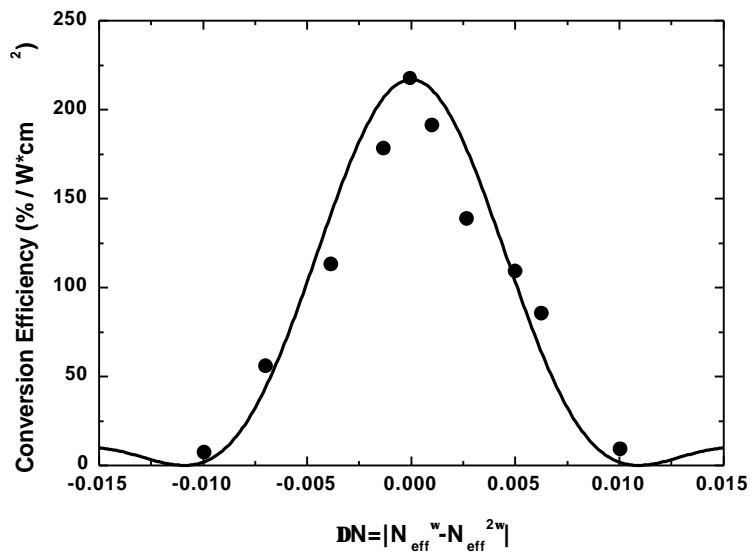
2



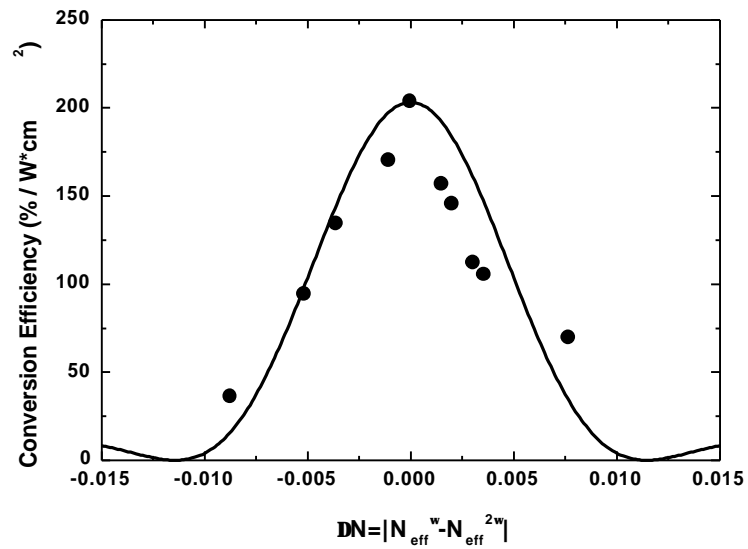
3



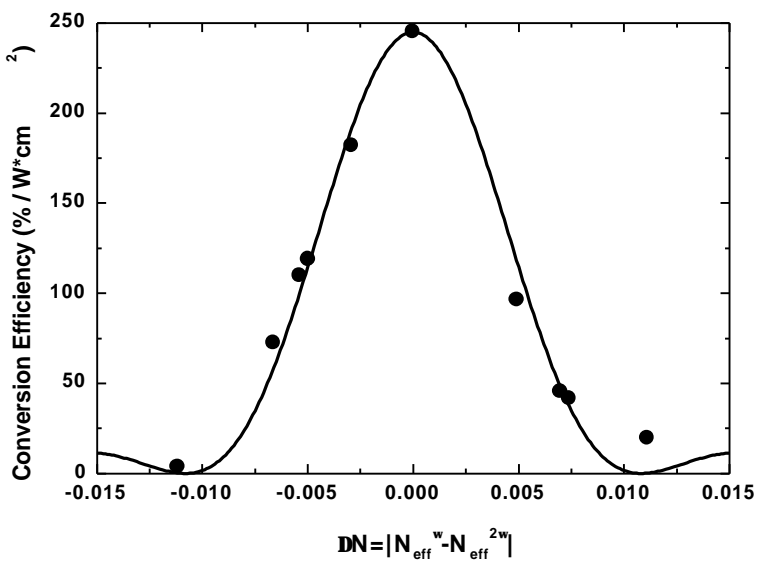
TBA



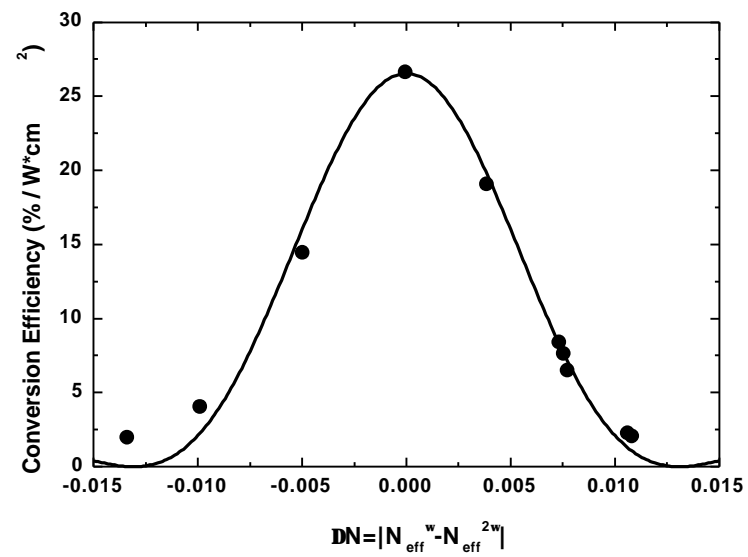
1



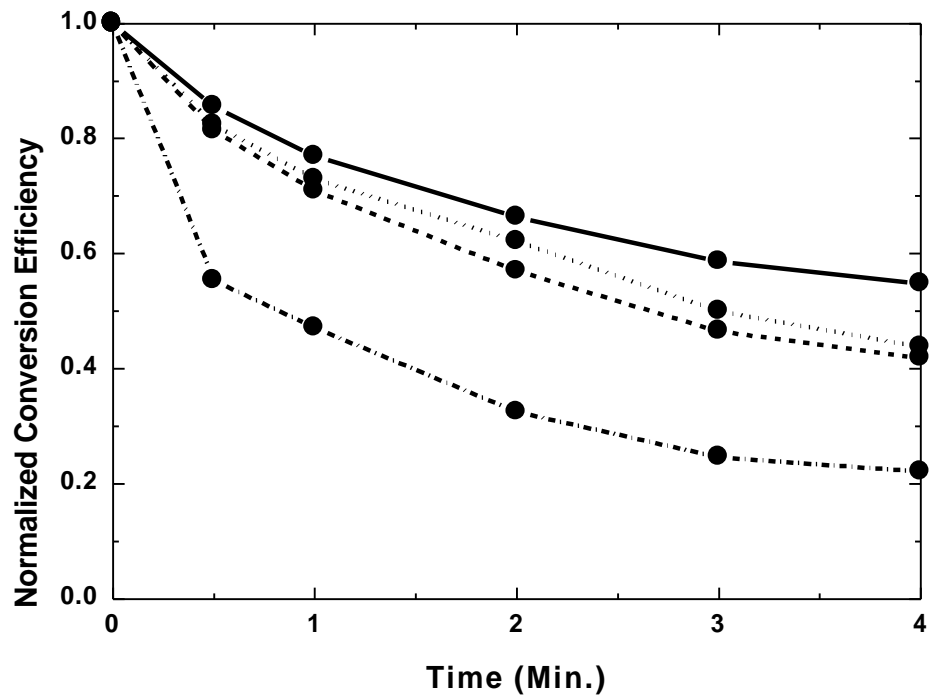
2



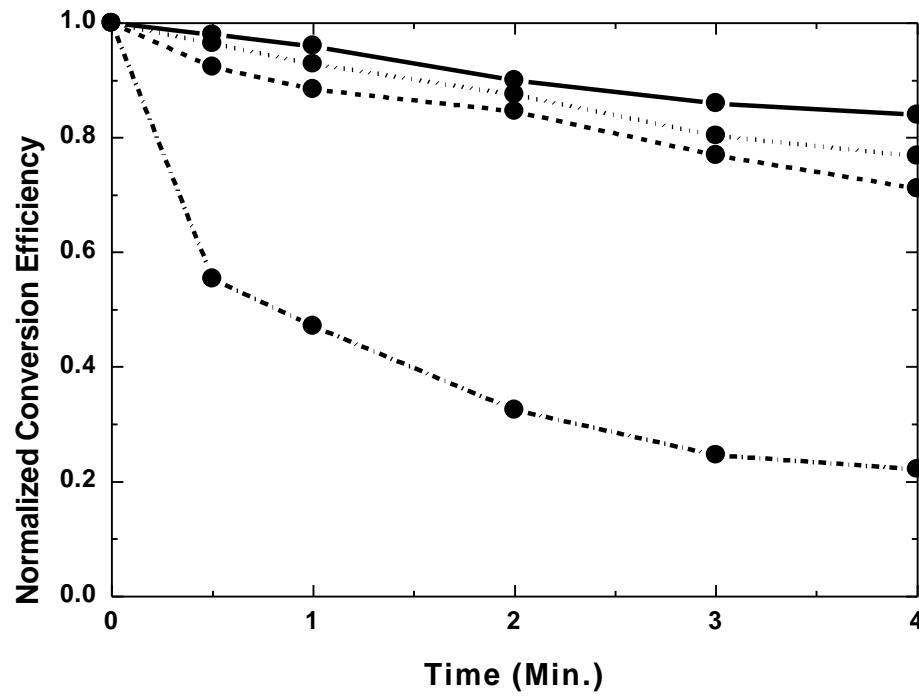
3



TBA



(a)



(b)

